Early quantitative profiling of differential retinal protein expression in lens-induced myopia in guinea pig using fluorescence difference two-dimensional gel electrophoresis

YI WU[1-3*], CARLY SIU-YIN LAM[2*], DENNIS YAN-YIN TSE[2,3*], CHI HO TO[1,2], QUAN LIU[1,2], SALLY A. McFADDEN[3], RACHEL KA-MAN CHUN[2], KING KIT LI[2], JIANFANG BIAN[2] and CHUEN LAM[2]

[1]State Key Laboratory of Ophthalmology, Zhongshan Ophthalmic Center, Sun Yat-Sen University, Guangzhou, Guangdong 510060; [2]Laboratory of Experimental Optometry, Centre for Myopia Research, School of Optometry, The Hong Kong Polytechnic University, Hong Kong, SAR, P.R. China; [3]School of Psychology, Faculty of Science and IT, The University of Newcastle, Callaghan, NSW 2308, Australia

Abstract. The current study aimed to investigate the differential protein expression in guinea pig retinas in response to lens-induced myopia (LIM) before fully compensated eye growth. Four days old guinea pigs (n=5) were subjected to -4D LIM for 8 days. Refractive errors were measured before and at the end of the lens wear period. Ocular dimensions were also recorded using high-frequency A-scan ultrasonography. After the LIM treatment, retinas of both eyes were harvested and soluble proteins were extracted. Paired retinal protein expressions in each animal were profiled and compared using a sensitive fluorescence difference two-dimensional gel electrophoresis. The quantitative retinal proteomes of myopic and control eye were analysed using computerised DeCyder software. Those proteins that were consistently changed with at least 1.2-fold difference (P<0.05) in the same direction in all five animals were extracted, trypsin digested and identified by tandem mass spectrometry. Significant myopia was induced in guinea pigs after 8 days of lens wear. The vitreous chamber depth in lens-treated eyes was found to be significantly elongated. Typically, more than 1,000 protein spots could be detected from each retina. Thirty-two of them showed differential expression between myopic and untreated retina. Among these proteins, 21 spots were upregulated and 11 were downregulated. Eight protein spots could be successfully identified which included β-actin, enolase 1, cytosolic malate dehydrogenase, Ras-related protein Rab-11B, protein-L-isoaspartate (D-aspartate) O-methyltransferase, PKM2 protein, X-linked eukaryotic translation initiation factor 1A and ACP1 protein. The present study serves as the first report to uncover the retinal 2D proteome expressions in mammalian guinea pig myopia model using a top-down fluorescent dyes labelling gel approach. The results showed a downregulation in glycolytic enzymes that may suggest a significant alteration of glycolysis during myopia development. Other protein candidates also suggested multiple pathways which could provide new insights for further study of the myopic eye growth.

Introduction

The ability to screen thousands of protein candidates using a proteomic approach has opened up many opportunities for high throughput study of global changes in protein expression. Fluorescence difference two-dimensional gel electrophoresis (2D DIGE) and mass spectrometry (MS) technology have greatly contributed to advancing research in understanding the aetiology and providing new therapeutic opportunities for many diseases. Compared to the traditional 2D electrophoresis with either Coomassie blue or silver stains, 2D DIGE has superior accuracy and repeatability in terms of identifying differential protein expressions with the help of an internal standard running in the same 2D gel. Recently, many proteomes of different ocular tissues have been profiled and cataloged as protein databases (1-3). These databases provide a platform for comparative analysis of protein expression or regulation among different species during differentiation and development.

Myopia, also known as short-sightedness, is a multifactorial disorder which is characterised by an excessive elongation of the eyeball. Although clinically well characterised, the

Correspondence to: Professor Chi Ho To, Laboratory of Experimental Optometry, Centre for Myopia Research, School of Optometry, The Hong Kong Polytechnic University, 6 Yuk Choi Road, Hung Hom, Hong Kong, SAR, P.R. China
E-mail: chi-ho.to@polyu.edu.hk

Professor Quan Liu, State Key Laboratory of Ophthalmology, Zhongshan Ophthalmic Center, Sun Yat-Sen University, 2 South Xianlie Road, Guangzhou, Guangdong 510060, P.R. China
E-mail: drliuquan@163.com

*Contributed equally

molecular mechanisms governing the accelerated ocular growth in myopia are still poorly understood. Experimental manipulations of visual experience affect eye growth and refractive status in many species such as chicks (4,5), tree shrews (6), fish (7), mice (8), monkeys (9), marmosets (10) and guinea pigs (11). In these studies, significant myopia can be induced when a growing eye wears either a diffuser (called form deprivation myopia) or a negative powered lens [called lens-induced myopia (LIM)]. In humans, myopia also accompanies diseases which cause visual deprivation, such as neonatal eye closure, ptosis, corneal opacity, or congenital cataract (12-15).

Although the exact mechanism(s) underlying myopia remains elusive, it is generally accepted that the retina can play a major role in modulating eye growth as a consequence of altered visual processing (16,17). This notion is supported by the evidence that eyes still respond to the defocus even with optic nerve sectioning (18,19). It implied the signals responsive to ocular development reside within the retina and no higher centre is required. It is believed that those biochemical signals initiated will then affect changes in the choroid and cause tissue remodelling in the sclera. This cascade results in exaggerated eye elongation and a myopic eyeball.

Proteomic approaches can provide snap-shots of the dynamic changes in cellular proteins during this process of myopic eye elongation. The chick has long been a popular animal model for myopia research due to a rapid and large dynamic response range to form deprivation and lenses. Retinal protein expression in chicks has been recently studied using a proteomic approach (20-22). Novel proteins which may be involved in the emmetropisation process as well as in myopia development were successfully identified. However, similar studies in myopic guinea pig retina are scarce (23) and no retinal protein profiles of pigmented guinea pigs exist. The guinea pig is a useful mammalian model of myopia due to the rapid and relatively reliable changes that can be induced and it has gained popularity in recent years. Therefore, the present study investigated the differential retinal protein expression in retinas extracted from myopic guinea pig eyes to provide insight into the retinal signalling pathways during myopia development.

Materials and methods

Animals. The animal setup was similar to our previous studies (24,25). Tri-coloured guinea pigs (Cavia porcellus) were raised in their natural litters with their mothers (each box was 65x45x20 cm) with open stainless wire lids. Lighting was provided by incandescent light bulbs (12x40 W) evenly dispersed through a 2 cm white Perspex barrier located 20 cm above each group of 4 boxes. The luminance was 400 lux at the centre of each box on a 12/12 h light/dark cycle. The room temperature was maintained at 21±2°C and humidity at 55±5%. Animal care was approved by the ethics committee of the University of Newcastle in accordance with Australian legislative requirements and the ARVO Statement for the Use of Animals in Ophthalmic and Vision Research.

Myopic tissue generation procedures. At 4 days of age, five guinea pigs wore a -4D lens monocularly for 8 days. Each lens was attached using hook and loop fastener as previously described (26). The fellow untreated eyes served as controls. At 12 days of age, both eyes were cyclopleged [with one drop of 1% cyclopentolate hydrochloride, Cyclogyl (Alcon Laboratories, Inc., Fort Worth, TX, USA)] and refractive error was measured 1 h later (without the -4D lens) using streak retinoscopy as previously described (27). Data are reported as the mean refractive error in the horizontal and vertical meridians. Animals were then anesthetised with isoflurane in oxygen, the -4D lens was removed, and ocular dimensions were measured in each eye using high-frequency A-scan ultrasonography. Details of the ultrasonography have been previously described (28). In summary, this procedure used a gel-coupled transducer (20 MHz, 1' focal length; Parametrics, Waltham, MA, USA) and signals were sampled at 100 MHz. Peaks were selected from the front of the cornea, the front and back of the lens, and the vitreous/retinal, RPE/choroidal, and choroidal/scleral interfaces and the back surface of the sclera. Ocular length was defined as the distance from the front surface of the cornea to the back of the sclera. After measurement of ocular parameters, anesthesia for the animal was ceased and the -4D lens was repositioned in front of the eye immediately.

Animals were then sacrificed by CO_2 overdose after 1 h of recovery. The eyes were rapidly enucleated and hemisected near to the equator. The anterior segment including the crystalline lens was removed together with the vitreous gel. Retinas were carefully peeled off from the posterior hemisphere without the retinal pigment epithelium attached. Any remaining retinal pigment epithelium was carefully removed by forceps. The retinas were immediately frozen in liquid nitrogen and stored at -80°C until used for protein analysis.

Extraction of retinal proteins. Similar to our previous study (20), each frozen retinal tissue was homogenised in a liquid nitrogen-cooled Teflon freezer mill (micro-dismembrator; Braun Biotech, Melsungen, Germany) with DIGE compatible lysis buffer containing 7 M urea, 2 M thiourea, 30 mM tris, 2% (w/v) CHAPS, 1% (v/v) ASB14 for 7 min at the highest speed. The homogenate was then centrifuged at 16,100 g for 15 min at 4°C. The supernatant (retinal protein extract) was collected and the pellet was discarded. The protein concentration of each retina was measured by a 2-D Quant kit according to manufacturer's instructions (GE Healthcare Life Sciences, Uppsala, Sweden).

Protein labelling. A 50 µg sample of protein from each treated and control retina was randomly labelled with either Cy3 or Cy5 while additional pooled protein samples were labelled with Cy2 as an internal standard (Table I). For each retina, the 50 µg of total protein was mixed with 1 µl of fresh dye solution (400 pmol/µl) and incubated in the dark for 30 min on ice. One µl of 10 mM lysine was then added and the sample incubated for a further 10 min to stop the labelling reactions. After labelling, the Cy3 and Cy5 labelled samples were mixed with the pooled Cy2 labelled samples and an equal volume of lysis buffer with 2% (w/v) DTT and 0.4% (v/v) Biolyte was added. The final volume for all preparations was adjusted to a total volume of 300 µl using rehydration buffer (7 M urea, 2 M thiourea, 2% CHAPS, 1% ASB14, 1% DTT, 0.2% Biolyte).

Table I. The experimental design of CyDye labelling for each individual retinal paired sample (n=5).

Gel no.	Cy2 dye (internal control)	Cy3 dye	Cy5 dye
Gel 1	Pool of all 10 eyes (5 μg from each sample)	Treated 1 (50 μg)	Control 1 (50 μg)
Gel 2	Pool of all 10 eyes (5 μg from each sample)	Control 2 (50 μg)	Treated 2 (50 μg)
Gel 3	Pool of all 10 eyes (5 μg from each sample)	Treated 3 (50 μg)	Control 3 (50 μg)
Gel 4	Pool of all 10 eyes (5 μg from each sample)	Control 4 (50 μg)	Treated 4 (50 μg)
Gel 5	Pool of all 10 eyes (5 μg from each sample)	Treated 5 (50 μg)	Control 5 (50 μg)

A total of 50 μg treated and un-treated control eyes were labelled with different dyes (Cy3 or Cy5 randomly). A total of 150 μg labelled proteins (treated, control and pooled standard) were loaded on each gel (gel 1-gel 5) for 2D difference gel electrophoresis run.

2-D gel electrophoresis. Isoelectric focusing (IEF) was performed using linear immobilised pH gradient (IPG) strips (pH 5-8, 17 cm; Bio-Rad Laboratories, San Diego, CA, USA). They were actively rehydrated at 50 V in Protean IEF cell (Bio-Rad Laboratories) under constant temperature (20˚C) for 12 h to enhance protein uptake. Subsequently, the protein samples were focused for a total of 30 k voltage-h (Vh). Following IEF, the IPG strips were incubated for 10 min in the equilibration buffer (6 M urea, 30% glycerol, 50 mM tris and 2% SDS) containing 2% DTT and then for an additional 10 min in 2.5% iodoacetamide. Afterwards, second dimension electrophoresis was conducted on 12% polyacrylamide gels casted in between low fluorescence Pyrex glass plate in the Protean II XL (Bio-Rad Laboratories) tank until completion. Both IEF and electrophoresis procedures were performed in the dark to avoid degradation of the Cy dyes.

DIGE gel image analysis. The images from the gels were scanned using a Typhoon 9400 Variable Mode Imager (GE Healthcare Life Sciences). The Cy2 image was scanned at an excitation wavelength of 488 nm and at an emission wavelength of 520 nm/BP 40 nm (maxima/bandwidth). The Cy3 image in the same gel was scanned at 532 nm (580 nm/BP 40 nm), while The Cy5 image in the same gel was scanned was at 633 nm (670 nm/BP 30 nm). The scan resolution was set at 100 μm.

All cropped DIGE gel images were analysed by the DeCyder Differential Analysis software, version 6.0 (GE Healthcare Life Sciences). All spot detection and matching according to the experimental design in Table I were performed automatically. Spots artefacts were screened using pre-set filters as reported (20). DeCyder biological variation analysis (BVA) was performed for pair-wise image analysis among all the five gels using the corresponding pooled internal standard Cy2 spot images from the same gel. The normalised ratios and Student's t-test of differentially expressed proteins were calculated by the software to compare the significant differences of protein abundance between the myopia and control eyes.

Protein identification and tandem MS. After scanning the gel images, gels were visualised with a MS compatible silver stain. The differentially expressed protein spots found by the software were then excised manually for in-gel digestion. Subsequent protein identifications were performed in two tandem MS systems.

For MALDI-TOF/TOF analysis, differentially expressed proteins were excised for in-gel trypsin digestion as described in our previous study (20). In brief, the analytes were mixed with α-cyano-4-hydroxycinnamic acid matrix solution. They are allowed to air-dry on an AnchorChip™ 600/384 (Bruker Daltonics, Bremen, Germany) Anchor target plate. Mass spectra were obtained on an AutoflexIII MALDI-TOF MS/MS mass spectrometer (Bruker Daltonics) under the positive ion reflectron mode with a 5-point nonlinear external calibration and internal trypsin autoproteolytic calibration. The resulting peak lists from 700 to 3,000 m/z for all samples were used to identify proteins from tryptic peptide fragments by utilising Uniprot and NCBI databases via the MASCOT protein database search engine.

For NanoLC-Electrospray MS/MS analysis, an UltiMate 3000™ NanoLC system coupled to a HCTultra ion trap mass spectrometer (Bruker Daltonics) was employed for protein identification. The tryptic in-solution digests in 0.1% (v/v) formic acid were injected onto a reversed-phase pre-column (C18 PepMap, 300 μm i.d., 5 mm; LC Packings, Amsterdam, The Netherlands) and then eluted on a nano reversed phase column (C18 PepMap, 75 μm i.d., 150 mm; LC Packings) with linear gradients from 96% mobile phase A/4% mobile phase B to 50% mobile phase A/50% mobile phase B in 10 min. The mobile phase A contained 0.1% (v/v) formic acid in water and mobile phase B contained 0.08% formic acid in water-ACN (20:80, v/v%). The column was connected to an electrospray emitter, distal coating, 20 μm i.d. with a 10 μm opening. The peptides were detected in the positive ion mode with a scan speed of 13,000 u/sec and fragmented by collision-induced dissociation. Precursor selection was set as 300-1,500 m/z. The two most abundant precursor ions were selected for MS/MS for each cycle. Three scans were averaged to obtain an MS/MS mass spectrum. The processing of the acquired MS data was triggered by a script for analysis by the DataAnalysisTM software (for chromatogram integration, mass annotation, and charge deconvolution) and subsequently the Biotools software (for protein database search on a MASCOT server).

In the database entry, we restricted the taxonomy to Metazoa (animals) and allowed a maximum of 1 missed cleavage. The potential chemical modifications of a peptide such as the alkylation of a cysteine [carbamidomethyl (C)] and the oxidation of a methionine residue [oxidation (M)] were also considered in the search. For all mass lists, no restrictions were applied for both the protein isoelectric point and molecular weight.

Data analysis. Biometric measures of refractive error and ocular dimension in treated and control eyes were compared using paired t-tests. Differences between the two eyes were calculated and referred to as 'relative' myopia or 'relative' ocular distances.

In order to screen the potential proteins related to myopia development and minimise false positive findings, stringent

Table II. Refractive errors and ocular component dimensions of guinea pigs after 8 days of -4D lens wear.

Sample type	Refractive errors (D)	ACD, mm	Lens thickness, mm	VCD, mm	Retinal thickness, mm	Choroidal thickness, mm	Scleral thickness, mm	Axial length, mm
Treated	-0.06±1.19[a]	1.198±0.031	3.141±0.028	3.074±0.020[b]	0.148±0.002[b]	0.084±0.009	0.089±0.005	7.734±0.079[a]
Control	+3.63±0.34	1.177±0.032	3.134±0.029	3.023±0.023	0.152±0.002	0.080±0.011	0.103±0.007	7.668±0.085

Data were presented as mean value ± standard error of the mean (mm except refractive errors). ACD and VCD denoted anterior chamber depth and vitreous chamber depth respectively. [a]P<0.05 (for refractive errors and axial length); [b]P<0.01 (for VCD and retinal thickness), paired t-test, n=5. ACD, anterior chamber depth; VCD, vitreous chamber depth.

criteria for defining differential protein expression were applied similarly to that previously described (20). The differentially expressed proteins had to be in the same direction of changes in all spot pairs with at least a 1.2-fold difference in the protein abundance between the treated and control eyes. We chose 1.2-fold difference as a threshold in another study so as to detect the maximum number of potential candidates at the reported sensitivity threshold of DIGE technique (29). Most importantly, the changes in spot abundance between treatment and control were required to reach statistical significance (P≤0.05, paired t-test). The ratio of each differentially expressed protein is shown as fold changes between samples from the myopic and control eye. The software allowed objective comparisons of the actual spots' intensities and profiles, and they are not altered by manual adjustments for contrast or brightness.

Results

Changes of refractive errors and ocular component dimensions. Significant relative myopia was induced in animals wearing a -4D lens for 8 days (treated vs. control, -0.06±1.19D vs. +3.63±0.34D, mean ± SEM, P<0.05). Treated eyes were found to have a longer mean vitreous chamber depth compared to that in their contralateral control eyes (P<0.01; Table II). Moreover, the mean axial length was significantly elongated relative to that in their untreated eyes (P<0.05; Table II). The retina was also relatively thinner (P<0.01). Other ocular component dimensions such as anterior chamber depth, lens thickness, and choroidal and scleral thicknesses remained unchanged (Table II). The control eyes showed a slight decrease in hyperopia as expected (before vs. after; +4.70±0.66D vs. +3.63±0.34D, P>0.05, n=5).

Protein spots image analysis. More than 1,000 protein spots could be detected on each gel typically. Thirty-two protein spots were differentially expressed in the myopic retina (Fig. 1) after gel analysis. Among them, 21 protein spots showed upregulation in abundance while 11 protein spots were downregulated in the eyes that had worn -4D lenses. Fig. 1 shows all differentially expressed proteins in an unadjusted gel image. Red spots indicated those downregulated proteins while blue spots were those upregulated proteins.

Protein identification and the reported functions. Of these 32 differentially expressed protein spots that were excised from

silver-post stained gels and underwent in-gel digestion followed by either MALDI-TOF MS/MS or nano LC ESI-MS/MS identifications. Eight of the isolated spots were successfully identified with the protein databases in Mascot server (P<0.01). The identities and general functions of these 8 are summarised in Table III. Corresponding images of each spot including the abundance change in individual animal and exact P-value between control and myopic eyes are shown in Fig. 2. Of the 8 proteins identified, 6 were significantly downregulated and 2 were significantly upregulated in abundance in every myopic retina relative to untreated contralateral eyes. Most of the proteins were small proteins in terms of molecular weights. Specific biological functions of these differentially expressed protein spots are described below.

Spot 1: β-actin. This protein is one of the non-muscle cytoskeletal actins isoforms in the actin family. Actins are highly conserved proteins which are essential for structural integrity of the body. β-actin is involved in cell motility and ATP binding. Downregulation of β-actin was also revealed in tree shrew sclera with LIM (30). Actin can be adhered to extracellular matrix which could be modified by growth process so as to provide biochemical and mechanical support to the cells.

Spot 2: Enolase 1. Enolase 1 is also known as α-enolase or non-neuronal enolase. It takes part in converting 2-phosphoglycerate to phosphoenolpyruvate during glycolysis. Deficiency of enolase causes generalised muscle weakness (31).

Spot 3: Cytosolic malate dehydrogenase. mRNA expression of Cytosolic malate dehydrogenase has a strong tissue-specific distribution, being expressed primarily in cardiac and skeletal muscle and in the brain, also at intermediate levels in the spleen, kidney, intestine, liver, and testes (32). It is known to participate in the malate-aspartate shuttle in the glycolysis process. The malate-aspartate shuttle mainly exists in the mitochondria of cells for translocating electrons produced during glycolysis with its primary roles related to aerobic energy production (such as for muscle contraction in other tissues). However, its role in the retina is not clear.

Spot 4: Ras-related protein Rab-11B (GTP-binding protein YPT3). The Rab family of proteins is a member of the Ras superfamily of monomeric G proteins. Rab GTPases regulate many steps of membrane trafficking including vesicle formation, vesicle movement along actin/tubulin networks,
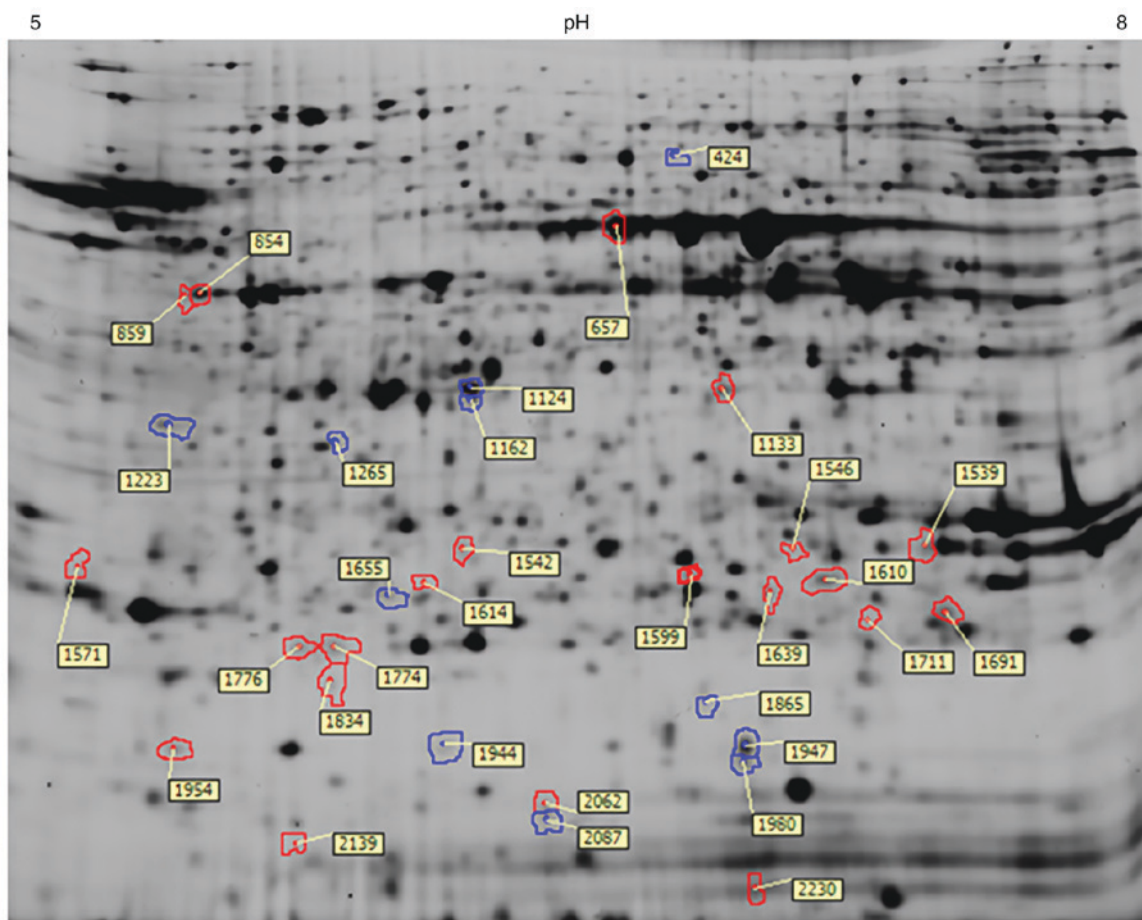
Figure 1. A representative difference gel electrophoresis gel image showing the locations of those differentially expressed proteins in guinea pig retinas after lens-induced myopia for 8 days. Spots in blue indicate upregulated proteins in myopic retina, while those in red indicate downregulated proteins. The number of each spot indicated the spot numbers used in the analysis of DeCyder software.

and membrane fusion. These processes make up the route by which cell surface proteins are trafficked from the Golgi to the plasma membrane and are recycled. Surface protein recycling returns proteins to the surface whose function involves carrying another protein or substance inside the cell, such as the transferrin receptor, or serves as a means of regulating the number of protein molecules on the surface. Rab11 plays a pivotal role in retinal development by regulating Shh signalling and mechanism acting in parallel with Shh signalling in the control of cell-cycle exit (33).

Spot 5: Protein-L-isoaspartate (D-aspartate) O-methyltransferase, PIMT. PIMT can methylate protein-L isoaspartate (D-aspartate). This protein participates in the MEK-ERK signal process, regulating cell proliferation and differentiation. PIMT gene knock-out mice show fatal seizures and developmental delay (34).

Spot 6: PKM2 protein. PKM2 protein is also named pyruvate kinase isoenzyme type M2. It is an isoenzyme of glycolytic enzyme pyruvate kinase. It catalyses the dephosphorylation of phosphoenolpyruvate to pyruvate with the production of ATP in the last step of glycolysis. A recent study showed that autoantibodies against PKM2 in serum may be a biomarker for age-related macular degeneration (AMD) (35). A higher level of anti-PKM2 IgG antibody was found in patients

with wet AMD compared to dry AMD (35). In rat retina, PKM2 has been reported to be present in the photoreceptors. Its enzymatic activity increased in dark-adapted retina suggesting a role in regulating the metabolism of photoreceptors (36).

Spot 7: X-linked eukaryotic translation initiation factor 1A. The main function of this factor is to help transfer Met-tRNAf to 40S ribosomal subunits to form a 40S pre-initiation complex (37,38). This complex translates mRNA to polypeptide in the process of protein synthesis. X-linked eukaryotic translation initiation factor 1A is required for cell growth in yeast (39).

Spot 8: ACP1 protein. ACP1 belongs to a family of low molecular weight acid phosphatase protein (LMW-PTP) which is a highly polymorphic phosphotyrosine-protein-phosphatase involved in signal transduction and cell proliferation control (40). In addition, LMW-PTP plays complex roles in the regulation of insulin (by dephosphorylating the insulin receptor), glucose, platelet derived growth factor receptor (PDGF), fibroblast growth factor (FGF) and T cell receptor signal transduction system (41). ACP1 genotype is also highly associated with retinopathy in diabetes mellitus type 2 patients as well as high body mass index and lipid levels (42).

Table III. A list of differentially expressed retinal proteins in response to –4D lens-induced myopia for 8 days.

Spot no.	DeCyder no. in Fig. 1	Protein name	Paired average ratio[a]	DeCyder P-value for fold change	MOWSE score[b]	NCBI GI no.[c]	Mascot cal. pI.[d]	Mascot Mw (kDa)[e]	Species[f]	Biological process	Molecular function
1	859	β-actin	-1.31	0.00042	294	49868	5.78	39.4	Mus musculus	Cell motility	i) ATP binding; ii) as cytoskeleton protein
2	657	Enolase 1	-1.22	0.003	481	87196501	6.37	47.6	Bos taurus	i) Glycolysis; ii) plasminogen activation	Catalysis of 2-phosphoglycerate to phosphoenolpyruvate during glycolysis
3	1133	Cytosolic malate dehydrogenase	-1.27	0.0034	165	55595921	7.57	38.9	Pan troglodytes	Oocyte maturation and embryo development	Malate-aspartate shuttle in glycolysis
4	1655	Ras-related protein Rab-11B/YPT3	+1.24	0.00028	391	763130	5.87	24.7	Homo sapiens	i) Protein transport; ii) small GTPase mediated signal transduction	i) GTP binding; ii) GTPase activity
5	1599	Protein-L-isoaspartate(D-aspartate) O-methyl transferase	-1.24	0.018	166	2507187	6.7	24.8	Homo sapiens	i) Protein amino acid methylation; ii) protein repair	i) Protein-L-isoaspartate (D-aspartate) O-methyltransferase activity
6	1639	PKM2 protein	-1.21	0.0091	155	73587283	8.62	62.0	Bos taurus	Glycolysis	i) Magnesium ion binding; ii) potassium ion binding; iii) protein binding; iv) pyruvate kinase activity
7	1954	X-linked eukaryotic translation initiation factor 1A	-1.24	0.00011	102	4503499	5.07	16.5	Homo sapiens	Translational initiation	Initiating translation activity
8	1947	pkm1 protein	+1.52	8.2e-005	256	74267860	6.71	18.6	Bos taurus	Protein amino acid dephosphorylation	i) Acid phosphatase activity; ii) non-membrane spanning protein tyrosine phosphatase activity

Proteins were identified by mass spectrometry with documented functions according to their GeneOntology. [a]Paired average ratio denotes fold difference between myopic and control retina. - and + indicate downregulation and upregulation in the myopic retina, respectively. [b]Score for the protein with significant match calculated by MOWSE scoring algorithm in the Mascot system. [c]A GI number is assigned to each nucleotide and protein sequence accessible through NCBI search systems. [d,e]Theoretical values of the isoelectric point and molecular weight obtained in the database search using Mascot system. [f]The species identified with the most significant score for a particular protein. MOWSE, Molecular Weight Search; NCBI, the National Centre for Biotechnology Information; GI, GenInfo Identifier; ACP1, adipocyte acid phosphatase; PKM2, pyruvate kinase PKM.
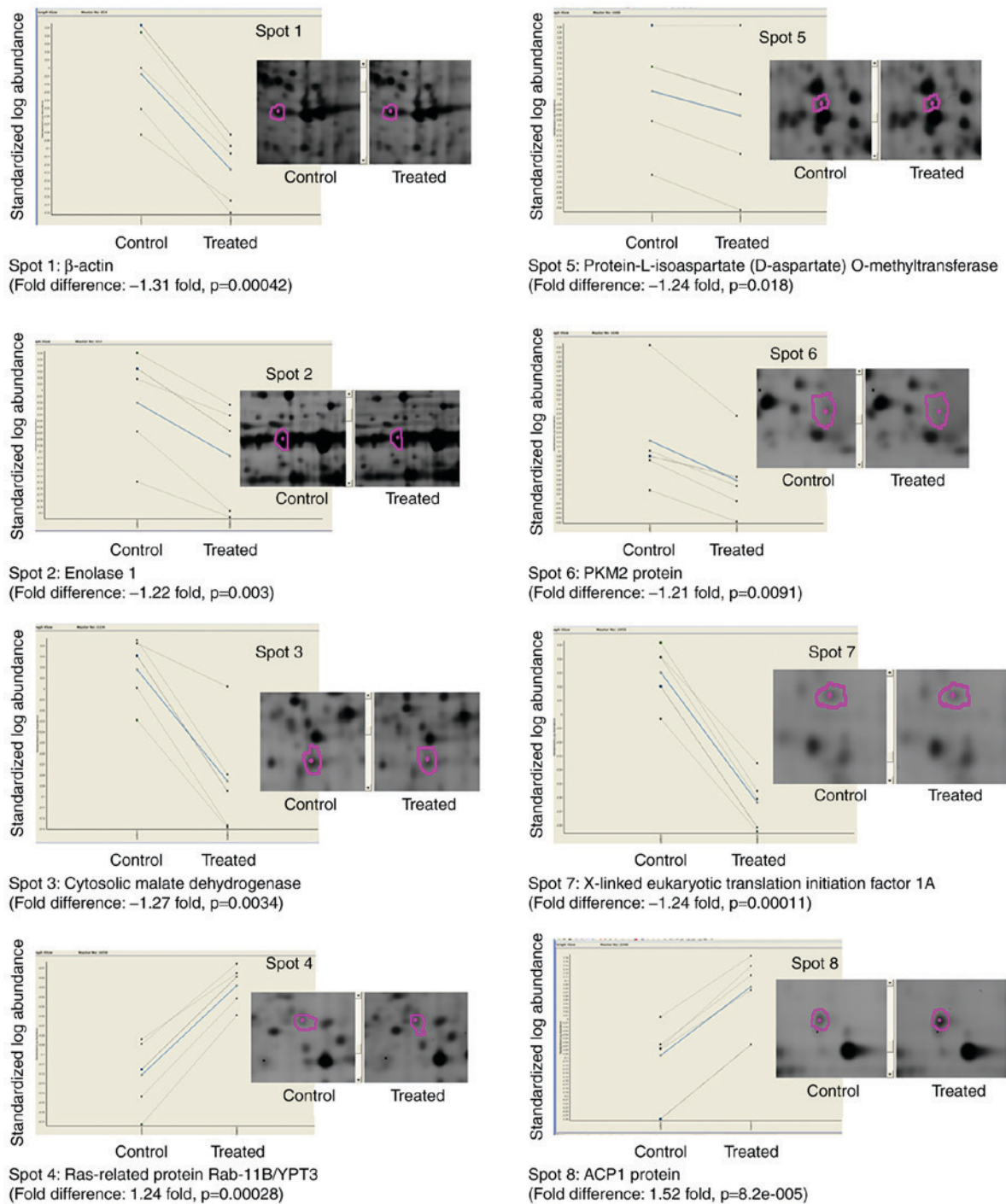
Figure 2. Differential protein expressions of the 8 proteins identified by tandem mass spectrometry with averaged fold changes and P-value shown. Solid lines represented averaged group expression while dotted lines denoted individual expression (n=5). The standardised log abundance of protein spot (y-axis) was plotted against control and treated retinas (x-axis). Purple circles indicate the boundaries of the protein spots automatically detected by the DeCyder Differential Analysis software. ACP1, adipocyte acid phosphatase; PKM2, pyruvate kinase PKM.

Discussion

There are a growing number of reports using guinea pig as a mammalian model for myopia research (27,43,44). The current study is the first to investigate the changes in retinal proteome in LIM in the guinea pig retina using 2D-DIGE coupled with MS. We started the treatment in young animals because they are more susceptible to the induced myopia. According to the lens compensation in response to -4D LIM in the pigmented guinea pigs (25), we chose 8 days as the treatment duration

which allowed the induction of relative, but not fully compensated, myopic eye growth. We intended to capture the early protein expressions which may be related to the early onset myopia. The induction of relative myopic eye growth using LIM approach was achieved in terms of both refractive error and axial length data. Using two different tandem MS systems, we have successfully identified a number of guinea pig retinal proteins which were differentially expressed in response to myopic eye growth. Of these differentially expressed proteins, three were downregulated: Enolase 1, cytosolic malate

dehydrogenase isoform 5 and PKM2 protein are all glycolysis-related enzymes which indicate a slowdown of glycolysis in accelerated ocular growth. The function of glycolysis is to oxidise glucose to pyruvate and produce ATP. Intuitively, one might have expected to observe an upregulation of glycolysis during accelerated eye growth because more ATPs would be required for ocular growth. Therefore, the observation is puzzling and exactly how downregulating glycolytic-related enzymes may lead to myopic eye growth is unknown. Further investigation is necessary to confirm if the glycolytic rate is indeed decreased in the myopic retina or whether it is due to the longer treatment period we used in this study. It is also noteworthy that single protein may process multiple biological functions and they could involve in other biochemical functions other than glycolysis. For example, multiple functional roles could be observed in PKM2. A number of studies have documented a specific function of PKM2 in tumour growth and spreading. The presence of the dimeric form of PKM2 in tumour cells may suggest it is associated with uncontrolled tissue growth (45,46). Apart from their conventional roles as reported in Table III, some of them were found associated with angiogenetic related processes. Reduced PKM2 at both mRNA and protein levels was found in retinal ischemia (47). Also, α-enolase, although traditionally considered a glycolytic enzyme, was suggested to promote plasminogen activation which is an important process in angiogenesis (48). Since high myopia is frequently associated with pro-angiogenic or neovascularization processes, it will be interesting to study the protein expressions of our reported proteins in the highly myopic eye. A recent genetic study on early-onset high myopia in children discovered mutation in a unique gene, BSG which encodes basigin (49). However, we could not identify basigin as a differentially expressed protein in our study. This could be due to relatively low myopia we induced in the present study. Also, this protein was reported to forms a complex with transporter in the retina so as to facilitate the nutrient transport across the membrane. It is difficult to study membrane proteins using our current protocol because of protein insolubility using gel based approach. In contrast, top-down proteomics strategy using high resolution liquid chromatography electrospray-ionization MS may be a better platform to study member proteins (50).

We are particularly interested in the novel role that enolase 1 may play in the myopia signalling cascades. The downregulation of enolase 1 was first reported in the myopic retina of guinea pigs in the present study. However, in our previous study, it was shown to be upregulated in guinea pig retina during recovery from LIM. These bi-directional changes of enolase 1 in both myopic and recovery retina strongly indicated the involvement of enolase 1 in myopia development (51). In addition, another isoenzyme of the same family, neuronal enolase was found to be associated with the severity of retinal detachment which is a common complication in myopic eyes (52,53).

Other than the changes of these glycolytic-related enzymes, there were upregulations of both ACP1 protein and YPT3. They are important proteins in cellular transport, signal translation or cell division. (33,40) These functions are clearly important during accelerated growth of the retina. Moreover, ACP1 was involved in the regulation of insulin which is recognised as strong myopia inducing factors in various reports (54,55). Hyperinsulinemia was also proposed to play a key role in the pathogenesis of juvenile-onset myopia (56). Hence, ACP1 signal transduction may be important in the biological cascade of reactions that constitute the clinical observation of susceptibility to myopia. They have also been the emerging targets for designing novel therapeutic agents in recent years because of their role in the phosphorylation of proteins which is fundamentally important to many cellular processes (57). The protein phosphorylation function of ACP1 highlights the importance of post-translational modification involving myopic eye growth.

Two novel proteins, PIMT and X-linked eukaryotic translation initiation factor 1A were differentially expressed in the retina from myopic eyes compared to control eyes. A recent study has suggested PIMT to be associated with visual and synapse development in guinea pigs (58). Abnormal visual signals may have stimulated excessive expression of Glutamate (NMDA) receptor subunit 1 in the retina which in turn led to the formation of myopia. While there is limited information on how X-linked eukaryotic translation initiation factor 1A may affect myopia development, another member of the same family, eukaryotic translation initiation factor 4H was shown to be downregulated in sclera's from myopic tree shrews (30). Although they are thought to be important in signalling and growth processes in other tissues, their exact biological functions in the retina need to be further explored.

Moreover, there was a study using a traditional 2DE approach to investigate the proteome changes in guinea pig sclera after 7 weeks of form deprivation. However, only a few differentially expressed proteins were found (59). The small number of protein changes could be due to the low sensitive staining method and short IPG strips used in that study. Comparing the differential expression in myopic sclera to our retinal data, no similarly expressed proteins were observed. The lack of shared protein changes may be due to different time points, ages and 2DE approach employed in different studies. Further studies are required to understand if there are very different biological reactions are at play in the retina and sclera.

Since introduction in 1997, the fluorescence difference 2D DIGE approach has been recognised as the most reliable gel-based proteomic approach for the detection of protein changes potentially associated with specific diseases (29,60). Owing to its property in employing multiple spectrally resolvable, size- and charge-matched fluorescent CyDye DIGE fluors for co-running up to three lysates in one single gel, more accurate protein profiling with consistent gel images could be achieved. Coupled with advanced gel analysis software, spot alignment, background subtraction as well as data normalisation could be automatically performed and calculated which allows minimal subjective assessment. Similar to our previous work in studying chick retinal samples using this DIGE approach (20), more than 1000 retinal protein spots could be typically resolved on a DIGE 2D gel in the pH range of 5-8. Aside from the number of protein spots, the retinal protein expressions in terms of global distribution on the 2D gels were also found to be very similar between the young guinea pig and chick. Nevertheless, only 32 of them were differentially expressed in response to the induced myopic eye growth in this study. In addition, only a limited number of interested

spots were successfully identified using two different types of MS analyses. The limitation on protein identification was mainly due to the low abundance of proteins. Although protein expression could be detected confidently with fluorescent CyDyes, the amount of protein was too low for subsequent MS analysis. Although we tried to increase the total protein loaded for 2DE, the 2D spot pattern was not distinct and optimal due to smearing effect. The relative higher cost in DIGE labelling for higher protein load was also of concern. This technical limitation was likewise observed in another proteomic study using chick retinal tissues (20). Therefore, a more sensitive MS system is required to reveal the identities of those low abundant proteins.

The study mainly focused on the expression of soluble proteins within pH 5-8 in which most of the retinal proteins can be resolved in a 2D DIGE gel as reported before (20). Hence, the retinal proteome examined in this study is not considered as fully comprehensive. Complementary work should extend into wider retina proteome coverage using bottom up shotgun proteomics using similar protocol or multiple treatment time points in order to capture more early signals. Also, the experimental setup of this study only focused in detecting treatment-induced effects between two eyes of the same animal instead of comparing protein changes to normal 'untreated' individual animal. It is still arguable sometimes whether the contralateral eye or 'un-touched' animal is a better 'control' in myopia research. Due to the known dynamic nature of protein expressions in retinal tissue during active growth, there would be greater inter-animal variations even in individuals with similar amount of refraction or ages (61). In order to minimise possible noises, we used paired eyes for comparative proteomics in this study. Using rather stringent criteria in screening differentially expressed proteins, the present study reported those that were detected in all guinea pigs in order to minimise false positive findings. Therefore, this study did not describe all the differences in retinal proteins during myopic growth and purposely excluded those proteins that failed to repeat in all of the five animals. Notwithstanding the potential importance of these 'excluded' proteins, this study first focused on those most significant and repeatable differences of protein abundance in the myopic retina. Although the actual number of proteins being regulated is likely under-estimated in the present study, we postulated that the protein candidates reported will be good starting points for generating hypotheses that can unravel the biochemical mechanisms implicated in the development of myopia. Related gene and protein expressions could be further validated in order to explore the underlying mechanism of myopia development. Due to the limited availability of specific antibodies for guinea pigs, multiple reaction monitoring (MRM) MS could be an alternative approach to conventional western blot analysis.

With the help of an efficient, target-free DIGE approach, we investigated the changes in the retinal proteome of guinea pig in response to LIM before full compensation. Identification and relative quantification of eight differentially expressed proteins helped understand the underlying mechanism of myopia development. A significant alteration of glycolysis in LIM was suggested based on three glycolytic-related enzymes found. The exact role of glycolysis during myopia development requires further investigation.

References

1. Markoulli M, Papas E, Cole N and Holden B: Differential gel electrophoresis of the tear proteome. Optom Vis Sci 89: E875-E883, 2012.
2. Joseph R, Srivastava OP and Pfister RR: Differential epithelial and stromal protein profiles in keratoconus and normal human corneas. Exp Eye Res 92: 282-298, 2011.
3. Chowdhury UR, Madden BJ, Charlesworth MC and Fautsch MP: Proteome analysis of human aqueous humor. Invest Ophthalmol Vis Sci 51: 4921-4931, 2010.
4. Tse DY, Lam CS, Guggenheim JA, Lam C, Li KK, Liu Q and To CH: Simultaneous defocus integration during refractive development. Invest Ophthalmol Vis Sci 48: 5352-5359, 2007.
5. Wallman J, Turkel J and Trachtman J: Extreme myopia produced by modest change in early visual experience. Science 201: 1249-1251, 1978.
6. Norton TT: Experimental myopia in tree shrews. Ciba Found Symp 155: 178-199, 1990.
7. Shen W, Vijayan M and Sivak JG: Inducing form-deprivation myopia in fish. Invest Ophthalmol Vis Sci 46: 1797-1803, 2005.
8. Barathi VA, Boopathi VG, Yap EP and Beuerman RW: Two models of experimental myopia in the mouse. Vision Res 48: 904-916, 2008.
9. Bradley DV, Fernandes A, Lynn M, Tigges M and Boothe RG: Emmetropization in the rhesus monkey (*Macaca mulatta*): Birth to young adulthood. Invest Ophthalmol Vis Sci 40: 214-229, 1999.
10. Troilo D, Nickla DL and Wildsoet CF: Form deprivation myopia in mature common marmosets (*Callithrix jacchus*). Invest Ophthalmol Vis Sci 41: 2043-2049, 2000.
11. Howlett MH and McFadden SA: Form-deprivation myopia in the guinea pig (*Cavia porcellus*). Vision Res 46: 267-283, 2006.
12. Robb RM: Refractive errors associated with hemangiomas of the eyelids and orbit in infancy. Am J Ophthalmol 83: 52-58, 1977.
13. O'Leary DJ and Millodot M: Eyelid closure causes myopia in humans. Experientia 35: 1478-1479, 1979.
14. Hoyt CS, Stone RD, Fromer C and Billson FA: Monocular axial myopia associated with neonatal eyelid closure in human infants. Am J Ophthalmol 91: 197-200, 1981.
15. Johnson CA, Post RB, Chalupa LM and Lee TJ: Monocular deprivation in humans: A study of identical twins. Invest Ophthalmol Vis Sci 23: 135-138, 1982.
16. Wallman J and Winawer J: Homeostasis of eye growth and the question of myopia. Neuron 43: 447-468, 2004.
17. Morgan IG: The biological basis of myopic refractive error. Clin Exp Optom 86: 276-288, 2003.
18. Wildsoet C and Wallman J: Choroidal and scleral mechanisms of compensation for spectacle lenses in chicks. Vision Res 35: 1175-1194, 1995.
19. Troilo D, Gottlieb MD and Wallman J: Visual deprivation causes myopia in chicks with optic nerve section. Curr Eye Res 6: 993-999, 1987.
20. Lam TC, Li KK, Lo SC, Guggenheim JA and To CH: Application of fluorescence difference gel electrophoresis technology in searching for protein biomarkers in chick myopia. J Proteome Res 6: 4135-4149, 2007.

21. Lam TC, Li KK, Lo SC, Guggenheim JA and To CH: A chick retinal proteome database and differential retinal protein expressions during early ocular development. J Proteome Res 5: 771-784, 2006.
22. Bertrand E, Fritsch C, Diether S, Lambrou G, Müller D, Schaeffel F, Schindler P, Schmid KL, van Oostrum J and Voshol H: Identification of apolipoprotein A-I as a 'STOP' signal for myopia. Mol Cell Proteomics 5: 2158-2166, 2006.
23. Wu Y, Liu Q, To CH, Li KK, Chun RKM, Yu JFJ and Lam TC: Differential retinal protein expressions during form deprivation myopia in albino guinea pigs. Curr Proteomics 11: 37-47, 2014.
24. Leotta AJ, Bowrey HE, Zeng G and McFadden SA: Temporal properties of the myopic response to defocus in the guinea pig. Ophthalmic Physiol Opt 33: 227-244, 2013.
25. Howlett MH and McFadden SA: Spectacle lens compensation in the pigmented guinea pig. Vision Res 49: 219-227, 2009.
26. McFadden SA, Tse DY, Bowrey HE, Leotta AJ, Lam CS, Wildsoet CF and To CH: Integration of defocus by dual power Fresnel lenses inhibits myopia in the mammalian eye. Invest Ophthalmol Vis Sci 55: 908-917, 2014.
27. Howlett MH and McFadden SA: Emmetropization and schematic eye models in developing pigmented guinea pigs. Vision Res 47: 1178-1190, 2007.
28. McFadden SA, Howlett MH and Mertz JR: Retinoic acid signals the direction of ocular elongation in the guinea pig eye. Vision Res 44: 643-653, 2004.
29. Tonge R, Shaw J, Middleton B, Rowlinson R, Rayner S, Young J, Pognan F, Hawkins E, Currie I and Davison M: Validation and development of fluorescence two-dimensional differential gel electrophoresis proteomics technology. Proteomics 1: 377-396, 2001.
30. Frost MR and Norton TT: Alterations in protein expression in tree shrew sclera during development of lens-induced myopia and recovery. Invest Ophthalmol Vis Sci 53: 322-336, 2012.
31. Comi GP, Fortunato F, Lucchiari S, Bordoni A, Prelle A, Jann S, Keller A, Ciscato P, Galbiati S, Chiveri L, *et al*: Beta-enolase deficiency, a new metabolic myopathy of distal glycolysis. Ann Neurol 50: 202-207, 2001.
32. Lo AS, Liew CT, Ngai SM, Tsui SK, Fung KP, Lee CY and Waye MM: Developmental regulation and cellular distribution of human cytosolic malate dehydrogenase (MDH1). J Cell Biochem 94: 763-773, 2005.
33. Muto A, Arai K and Watanabe S: Rab11-FIP4 is predominantly expressed in neural tissues and involved in proliferation as well as in differentiation during zebrafish retinal development. Dev Biol 292: 90-102, 2006.
34. Kim E, Lowenson JD, Clarke S and Young SG: Phenotypic analysis of seizure-prone mice lacking L-isoaspartate (D-aspartate) O-methyltransferase. J Biol Chem 274: 20671-20678, 1999.
35. Morohoshi K, Ohbayashi M, Patel N, Chong V, Bird AC and Ono SJ: Identification of anti-retinal antibodies in patients with age-related macular degeneration. Exp Mol Pathol 93: 193-199, 2012.
36. Lindsay K, Linton J and Hurley J: Unique expression and regulation of glycolytic enzyme PKM2 in photoreceptor cells and the role of enzymatic activity modulating metabolism of the retina. Invest Ophthalmol Vis Sci 54: 692, 2013.
37. Chaudhuri J, Si K and Maitra U: Function of eukaryotic translation initiation factor 1A (eIF1A) (formerly called eIF-4C) in initiation of protein synthesis. J Biol Chem 272: 7883-7891, 1997.
38. Majumdar R, Bandyopadhyay A and Maitra U: Mammalian translation initiation factor eIF1 functions with eIF1A and eIF3 in the formation of a stable 40 S preinitiation complex. J Biol Chem 278: 6580-6587, 2003.
39. Kainuma M and Hershey JW: Depletion and deletion analyses of eucaryotic translation initiation factor 1A in *Saccharomyces cerevisiae*. Biochimie 83: 505-514, 2001.
40. Chiarugi P, Taddei ML, Schiavone N, Papucci L, Giannoni E, Fiaschi T, Capaccioli S, Raugei G and Ramponi G: LMW-PTP is a positive regulator of tumor onset and growth. Oncogene 23: 3905-3914, 2004.
41. Iannaccone U, Bergamaschi A, Magrini A, Marino G, Bottini N, Lucarelli P, Bottini E and Gloria-Bottini F: Serum glucose concentration and ACP1 genotype in healthy adult subjects. Metabolism 54: 891-894, 2005.
42. Lucarini N, Bottini N, Antonacci E, Borgiani P, Faggioni G and Gloria-Bottini F: Diabetic complications and the genetics of signal transduction. A study of retinopathy in NIDDM. Dis Markers 13: 169-176, 1997.
43. Lu F, Zhou X, Jiang L, Fu Y, Lai X, Xie R and Qu J: Axial myopia induced by hyperopic defocus in guinea pigs: A detailed assessment on susceptibility and recovery. Exp Eye Res 89: 101-108, 2009.
44. Lu F, Zhou X, Zhao H, Wang R, Jia D, Jiang L, Xie R and Qu J: Axial myopia induced by a monocularly-deprived facemask in guinea pigs: A non-invasive and effective model. Exp Eye Res 82: 628-636, 2006.
45. Mazurek S, Boschek CB, Hugo F and Eigenbrodt E: Pyruvate kinase type M2 and its role in tumor growth and spreading. Semin Cancer Biol 15: 300-308, 2005.
46. Mazurek S: Pyruvate kinase type M2: A key regulator of the metabolic budget system in tumor cells. Int J Biochem Cell Biol 43: 969-980, 2011.
47. Tan SQ, Geng X, Liu JH, Pan WH, Wang LX, Liu HK, Hu L and Chao HM: Xue-fu-Zhu-Yu decoction protects rats against retinal ischemia by downregulation of HIF-1α and VEGF via inhibition of RBP2 and PKM2. BMC Complement Altern Med 17: 365, 2017.
48. López-Alemany R, Longstaff C, Hawley S, Mirshahi M, Fábregas P, Jardí M, Merton E, Miles LA and Félez J: Inhibition of cell surface mediated plasminogen activation by a monoclonal antibody against alpha-Enolase. Am J Hematol 72: 234-242, 2003.
49. Jin ZB, Wu J, Huang XF, Feng CY, Cai XB, Mao JY, Xiang L, Wu KC, Xiao X, Kloss BA, *et al*: Trio-based exome sequencing arrests de novo mutations in early-onset high myopia. Proc Natl Acad Sci USA 114: 4219-4224, 2017.
50. Souda P, Ryan CM, Cramer WA and Whitelegge J: Profiling of integral membrane proteins and their post translational modifications using high-resolution mass spectrometry. Methods 55: 330-336, 2011.
51. Chun RKM, Tse DYY, Zuo B, Li KK, Zhang G, Liu Q, Zhang SA and To CH: Proteome analysis of guinea pig retina during recovery from lens-induced myopia: Invest Ophthalmol Vis Sci 52: 5646, 2011.
52. Dunker S, Sadun AA and Sebag J: Neuron specific enolase in retinal detachment. Curr Eye Res 23: 382-385, 2001.
53. Quintyn JC, Pereira F, Hellot MF, Brasseur G and Coquerel A: Concentration of neuron-specific enolase and S100 protein in the subretinal fluid of rhegmatogenous retinal detachment. Graefes Arch Clin Exp Ophthalmol 243: 1167-1174, 2005.
54. Feldkaemper MP, Neacsu I and Schaeffel F: Insulin acts as a powerful stimulator of axial myopia in chicks. Invest Ophthalmol Vis Sci 50: 13-23, 2009.
55. Tarutta E, Chua WH, Young T, Goldschmidt E, Saw SM, Rose KA, Smith E III, Mutti DO, Ashby R, Stone RA, *et al*: Myopia: Why study the mechanisms of myopia? Novel approaches to risk factors signalling eye growth-how could basic biology be translated into clinical insights? Where are genetic and proteomic approaches leading? How does visual function contribute to and interact with Ametropia? Does eye shape matter? Why Ametropia at all? Optom Vis Sci 88: 404-447, 2011.
56. Cordain L, Eaton SB, Brand Miller J, Lindeberg S and Jensen C: An evolutionary analysis of the aetiology and pathogenesis of juvenile-onset myopia. Acta Ophthalmol Scand 80: 125-135, 2002.
57. Maccari R and Ottanà R: Low molecular weight phosphotyrosine protein phosphatases as emerging targets for the design of novel therapeutic agents. J Med Chem 55: 2-22, 2012.
58. Liu SZ, Wen D, Mao JF, Tan XP, Xia ZH and Fu CY: The expression of NMDAR1 in the retina of guinea pigs with form-deprivation myopia. Chin J Optom Ophthalmol 10: 1-5, 2008 (In Chinese).
59. Zhou X, Ye J, Willcox MD, Xie R, Jiang L, Lu R, Shi J, Bai Y and Qu J: Changes in protein profiles of guinea pig sclera during development of form deprivation myopia and recovery. Mol Vis 16: 2163-2174, 2010.
60. Unlu M, Morgan ME and Minden JS: Difference gel electrophoresis: A single gel method for detecting changes in protein extracts. Electrophoresis 18: 2071-2077, 1997.
61. Lam TC, Chun RK, Li KK and To CH: Snapshots for intra-and inter-ocular differences at retinal proteins levels. Int J Ophthalmol Eye Res 2: 70-76, 2014.